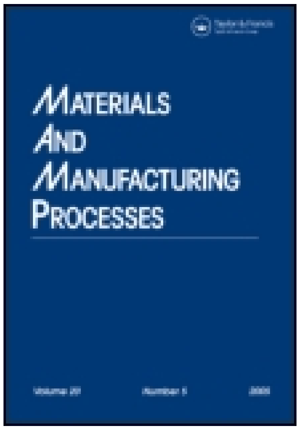

Materials and Manufacturing Processes
Publication details, including instructions for authors and subscription information:
http://www.tandfonline.com/loi/lmmp20

Synthesizing Nanostructured $Ni_{75}Mg_{16.66}Y_{8.34}$ (at%) Powder by Solid State Reaction and Mechanical Milling

S. Raygan [a] , M. Pourabdoli [a] , H. Abdizadeh [a] & M. Medraj [b]

[a] School of Metallurgy and Materials Engineering, College of Engineering, University of Tehran, Tehran, Iran

[b] Department of Mechanical and Industrial Engineering, Concordia University, Montreal, Quebec, Canada

Accepted author version posted online: 04 Sep 2012.Version of record first published: 26 Nov 2012.

To cite this article: S. Raygan , M. Pourabdoli , H. Abdizadeh & M. Medraj (2012): Synthesizing Nanostructured $Ni_{75}Mg_{16.66}Y_{8.34}$ (at%) Powder by Solid State Reaction and Mechanical Milling, Materials and Manufacturing Processes, 27:12, 1300-1305

To link to this article: http://dx.doi.org/10.1080/10426914.2012.663144

Materials and Manufacturing Processes, 27: 1300–1305, 2012

ISSN: 1042-6914 print/1532-2475 online
DOI: 10.1080/10426914.2012.663144

Synthesizing Nanostructured $Ni_{75}Mg_{16.66}Y_{8.34}$ (at%) Powder by Solid State Reaction and Mechanical Milling

S. Raygan[1], M. Pourabdoli[1], H. Abdizadeh[1], and M. Medraj[2]

[1]*School of Metallurgy and Materials Engineering, College of Engineering, University of Tehran, Tehran, Iran*
[2]*Department of Mechanical and Industrial Engineering, Concordia University, Montreal, Quebec, Canada*

In this study, nanostructured $Ni_{75}Mg_{16.66}Y_{8.34}$ (at%) catalyst powder was prepared using two methods. In method one, the pure elemental powders were subjected to high energy ball milling for 5 to 25 h with a ball to powder weight ratio of 20. In method two, the pure elemental powders were pressed, heat treated at 800°C for 8 h (solid state reaction); then, they were ball milled for 2, 7.5 and 10 h, similarly to the first method. Finally, morphology, phases, particle size, crystallite size, and lattice strain values of the prepared powder alloys were determined by X-ray diffraction (XRD) and scanning electron microscope (SEM) methods. The XRD patterns showed that the Mg_2Ni_9Y ternary intermetallic phase was not formed in the sample prepared by method one; however, that was formed in the samples prepared by the second method. The required milling time for preparing the samples with the same powder specifications by method two was about 50% less than the time required by method one. It was found that the $Ni_{75}Mg_{16.66}Y_{8.34}$ (at%) powder with smaller particle size, smaller crystallite size, and higher lattice strain values could be prepared by combining solid state reaction and mechanical milling processes.

Keywords Catalyst; Heating; Hydrogen; Intermetallics; Materials; Mechanochemistry; Milling; Nanocrystalline.

Introduction

Mechanical alloying is a powder processing technique which has been used to synthesize both equilibrium and metastable phases of commercially useful and scientifically interesting materials [1]. Non-equilibrium processing of materials has attracted the attention of a number of scientists and engineers due to the possibility of producing better and improved materials compared with the ones produced by conventional methods [1–3]. In solid state reaction process, the pressed pure elemental powders are subjected to heat treatment process involving specific temperature and time regimes [4].

Preparation of the alloys such as $Ni_{75}Mg_{16.66}Y_{8.34}$ (at%) which contain elements with high vapor pressure is difficult by conventional melting methods, such as vacuum arc melting and vacuum induction melting, and needs special facilities because of Mg vaporization and Y oxidation. However, the alloys can be synthesized either by combining mechanical milling and solid state reaction processes or by either one without any loss of elements due to evaporation [1–4].

Some specifications such as phase composition, particle sizes, and crystallite sizes are the main important specifications of catalysts that strongly change catalytic performance [5, 6]. Ni-based alloy powders are well-known catalysts in solid state hydrogen storage materials such as MgH_2 [7, 8].

Nanostructured $Ni_{75}Mg_{16.66}Y_{8.34}$ powder can be used as a catalyst for improving the hydrogen sorption properties of solid state hydrogen storage materials such as MgH_2. Some researchers [4, 9–13] have reported the preparation and structural determination of $Ni_{75}Mg_{16.66}Y_{8.34}$ and the similar alloys containing Mg and Y; but the nanostructured $Ni_{75}Mg_{16.66}Y_{8.34}$ (at%) powder prepared by solid state reaction and mechanical milling has not been reported yet.

The aim of this study was to prepare $Ni_{75}Mg_{16.66}Y_{8.34}$ powder using the mechanical alloying process and combining mechanical milling and solid state reaction processes; then, the structures, particle sizes, and crystallite sizes of the powder as the main important specifications of a catalyst prepared by the two methods were studied and compared.

Experimental

Materials

Pure elemental powders of Mg (Bayer Germany, <63 µm, 99.95%), Ni (Inco Canada, <10 µm, 99.97%), and Y (Ukraine, <0.5 mm, 99.95%) were used for the experiments.

Sample Preparation

Two methods were used for preparing the $Ni_{75}Mg_{16.66}Y_{8.34}$ (at%) powder. In method one, the samples were prepared only by the mechanical alloying process, while, in method two, they were prepared by combining solid state reaction and ball milling processes. The used methods are explained as follows.

Mechanical alloying. According to $Ni_{75}Mg_{16.66}Y_{8.34}$ (at%), 10 g powder mixture was prepared from pure elemental powders; then, it was mechanically milled

Received October 15, 2011; Accepted January 13, 2012

Address correspondence to S. Raygan, School of Metallurgy and Materials Engineering, College of Engineering, University of Tehran, Tehran, Iran.; E-mail: shraygan@ut.ac.ir

under argon atmosphere (0.1 Mpa) for 0, 5, 10, 20, and 25 h with a ball to powder weight ratio of 20 and rotating speed of 250 rpm in a planetary ball mill.

Combining solid state reaction and mechanical milling processes. Ten grams primary pure elemental powders were mixed according to the stoichiometric ratios of $Ni_{75}Mg_{16.66}Y_{8.34}$ (at%); then, they were pressed as a cylindrical tablet with the diameter of 25 mm, thickness of 4.24 mm, and density of 4.8 g/cm^3. The tablet was located in the steel vacuum vessel and heated to 800°C in the muffle furnace for 8 h in order to perform solid state reaction. Then, the heat treated tablets were milled for 2, 7.5, and 10 h.

Characterization

X-ray powder diffraction was carried out using a *Philips X'Pert Pro* diffractometer with CuK_α radiation and mean crystallite size and lattice strains were calculated using the Williamson–Hall procedure [14]. The morphology of the prepared powders and particle sizes were studied by scanning electron microscopy (*Cam Scan MV2300*). The phase identification, mean crystallite size, and lattice strain values were determined by *Match Crystal Impact* (version 1.9a) and *X'Pert HighScore* (version 1.0d) software.

Results and discussion

Phase Composition

Figure 1 [12] and Table 1 [15] show the Ni-Mg-Y ternary diagram section and phase regions at 673 K. The Ni-rich corner of the Mg-Ni-Y system has 9 binary intermetallics, which are $Ni_{17}Y_2$, Ni_5Y, Ni_4Y, Ni_3Y, Ni_2Y, NiY, Ni_2Y_3, $MgNi_2$, and Mg_2Ni. Moreover, the system

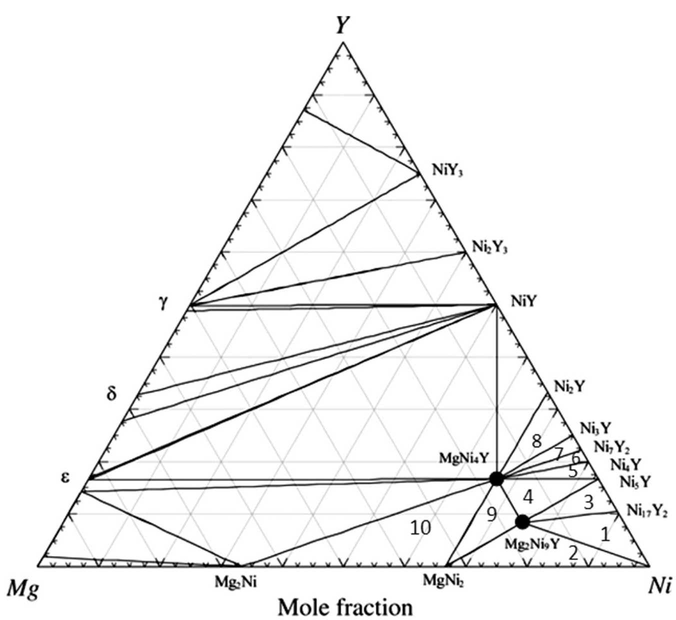

FIGURE 1.—Isothermal section of the Ni-Mg-Y ternary system at 673 K [12].

TABLE 1.—Three phase regions of the Mg-Ni-Y ternary system (Ni-rich corner) at 673 K [15].

Region number	Phase composition
1	Ni $+Y_2Ni_{17}$ $+YM_2Ni_9$
2	Ni $+MgNi_2$ $+YMg_2Ni_9$
3	Y_2Ni_{17} $+YNi_5$ $+YMg_2Ni_9$
4	YNi_5 $+YMg_2Ni_9$ $+YMgNi_4$
5	$YMgNi_4$ $+YNi_4$ $+YNi_5$
6	$YMgNi_4$ $+YNi_4$ $+Y_2Ni_7$
7	$YMgNi_4$ +Y2Ni$_7$ $+YNi_3$
8	$YMgNi_4$ $+YNi_3$ $+YNi_2$
9	$YMgNi_4$ $+YMg_2Ni_9$ $+YNi_2$
10	$YMgNi_4$ $+MgNi_2$ $+Mg_2Ni$

has two ternary intermetallics, i.e., Mg_2Ni_9Y (A) and $MgNi_4Y$ (B) in the Ni-rich corner [15].

There are three phase regions of ϵ-$Mg_{24}Y_{5-x}$, δ-Mg_{2-1-x} and γ-MgY_{1-x} in the Mg-Y binary system [16, 17]. The possibility of forming these phases in this study was very low because the dominant element in the powder mixture was Ni (79.35 wt%) and the amounts of the used Mg (7.30 wt%) and Y (13.35 wt%) elements were not large enough to form a significant amount of the above-mentioned binary intermetallics.

The X-ray patterns of the samples prepared only by the mechanical alloying process are shown in Fig. 2. In this figure, the peaks of Mg_2Ni_9Y or other ternary or binary phases are not seen or distinguished, but the Ni, Mg, and Y peaks are seen, and their intensities are decreased and broaden with milling time. Mg peaks intensities decreased after 5 h of mechanical alloying, while Y peaks were yet visible. This case could be originated from primary particle sizes and brittle or ductile nature of raw materials. Y is more ductile than Mg. Also, primary Y wt% value and powder particles (<0.5 mm) were larger than primary Mg powder particles (<63 μm); therefore, more milling time was needed for decreasing the particles size and peak broadening of Y compared with those of Mg. Moreover, non-uniform lattice strains and compositional variations changed *d*-spacing and influenced the peak width.

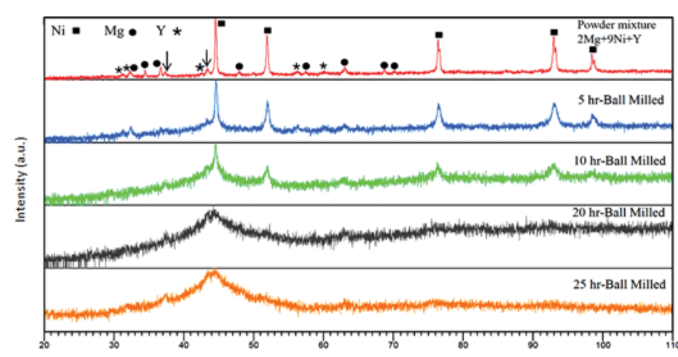

FIGURE 2.—XRD patterns of the powders prepared by mechanical alloying (arrows show NiO peaks as impurity) (color figure available online).

Further mechanical alloying time up to 10 h led to the disappearance of the Mg and Y peaks, which demonstrated the reaction between Ni, Mg, and Y and the formation of binary and ternary phases. The amount of formed phases was negligible due to the small amounts of Mg and Y in the primary powder. Therefore, the phase peaks of the evolved phases were very weak and were not identifiable in the patterns. Moreover, crystallite sizes decreased by the increment of the milling time, which led to broadening and overlapping the peaks and further difficult phase identification. Amorphous phase was formed with mechanical milling of the powder for more than 20 h. This phenomenon could be seen in the X-ray diffraction (XRD) pattern of the powder as a broadened peak. Amorphization by mechanical milling is the result of inducing energy and introducing the defects into the crystal structure by mechanical impacts.

Figure 3 shows the XRD patterns of the samples prepared by combining solid state reaction and ball milling processes. According to Fig. 3, the Mg_2Ni_9Y, YNi_5, Y_2Ni_{17}, YNi_2, and YNi_4 phases may be formed during the solid reaction process. Ball milling of the solid state partially-reacted sample for 2 h broadened the peaks of Mg_2Ni_9Y, YNi_5, and YNi_4 and disappeared the YNi_2 peaks. Probably, the decomposition of the YNi_2 during the ball milling was the reason for the disappearance of its peaks. According to XRD patterns for the 10 h milled powder, the present phases were Ni, Mg_2Ni_9Y, YNi_5, and Y_2Ni_{17}. The comparison of the formed phases with the phase regions in Fig. 1 showed that, after 10 h of ball milling, the system was not in the equilibrium state.

The formed phases in the samples can be very important in view of the catalytic effects on the hydrogen sorption because different phases have different catalytic effects.

Particle Size

Figure 4 shows the scanning electron microscopy (SEM) pictures of the powders prepared by only mechanical alloying. It can be seen that the particle sizes were in the range of 5 to 20 μm after 20 h of ball milling. Further ball milling up to 25 h caused the agglomeration

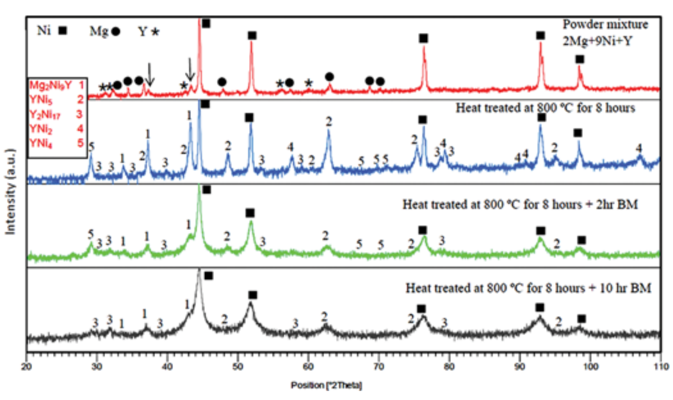

FIGURE 3.—XRD patterns of the samples prepared by combining solid state reaction and ball milling processes (arrows show NiO peaks as impurity) (color figure available online).

of the particles so that their morphology changed and sizes increased to 15 to 30 μm. Moreover, the particles produced by only the mechanical alloying process mainly had round corners due to the ductile nature of primary powders, i.e., Ni and Y. The size of the catalyst particles is an important parameter in its performance because a catalyst with the smaller particle sizes is distributed uniformly in the metal surface and provides more sites for catalytic reaction. Therefore, mechanical alloying for 20 h is the optimum time for providing the powders with smaller particle sizes.

Figure 5 shows the SEM images of the ball milled samples prepared by solid state reaction. Herein, the particle sizes of the primary powder were in the range of 20 to 300 μm, while the size reached approximately 2 to15 μm after 10 h of ball milling. Some agglomerated particles can be observed in this figure.

The particles produced by combining solid state reaction and ball milling processes had sharp corners due to the brittle nature of intermetallic compounds formed during solid state reaction. The sharp corners are suitable sites for initiating the gas sorption reactions; in addition, the particles with sharp corners have larger surface areas than the round corner particles [5, 6].

Particle size is an important factor in a catalyst performance, especially the catalysts which are used for improving the hydriding properties of the solid state hydrogen storage materials. Higher surface areas are created due to decreasing the particle sizes and can improve the reaction kinetics.

Crystallite Size and Lattice Strain Values

The crystallite size of the powder was estimated from the broadening of the peaks in the XRD patterns of Ni using the Williamson–Hall method according to the following equation:

$$\beta = 2\varepsilon \tan\theta + \lambda/\mathrm{d}\cos\theta, \tag{1}$$

where β is the full width half maximum of each peak at the Bragg angle of θ, λ is the X-ray wavelength, d is the crystallite size, and ϵ is the lattice strain [14].

The phases formed during the mechanical alloying process were not identifiable in the XRD patterns due to their very low contents and very weak peaks in the XRD patterns. Also, the peaks originated from the phases formed during the ball milling of the solid reacted sample are complicated and, in many cases, overlapped. Hence, it was not possible to calculate the crystallite sizes of the evolving phases by the Williamson–Hall procedure. Therefore, only the crystallite sizes of Ni particles and lattice strain values were calculated in both cases due to the strong peak intensities in the XRD patterns.

Table 2 shows the specifications of the powders prepared by both methods. It is evident that the mean crystallite size decreased while lattice strain values increased with increasing the ball milling time in both preparation methods. It is notable that the mean crystallite size of the powders produced by combining solid state reaction

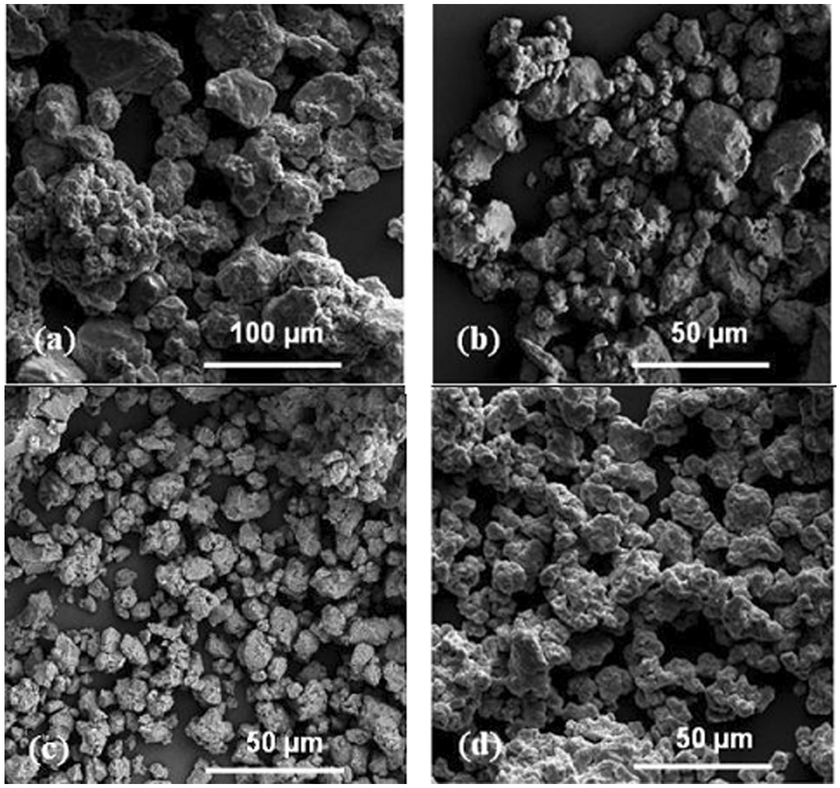

FIGURE 4.—SEM images of the powders prepared by mechanical alloying: a) 5 h, b) 10 h, c) 20 h, and d) 25 h.

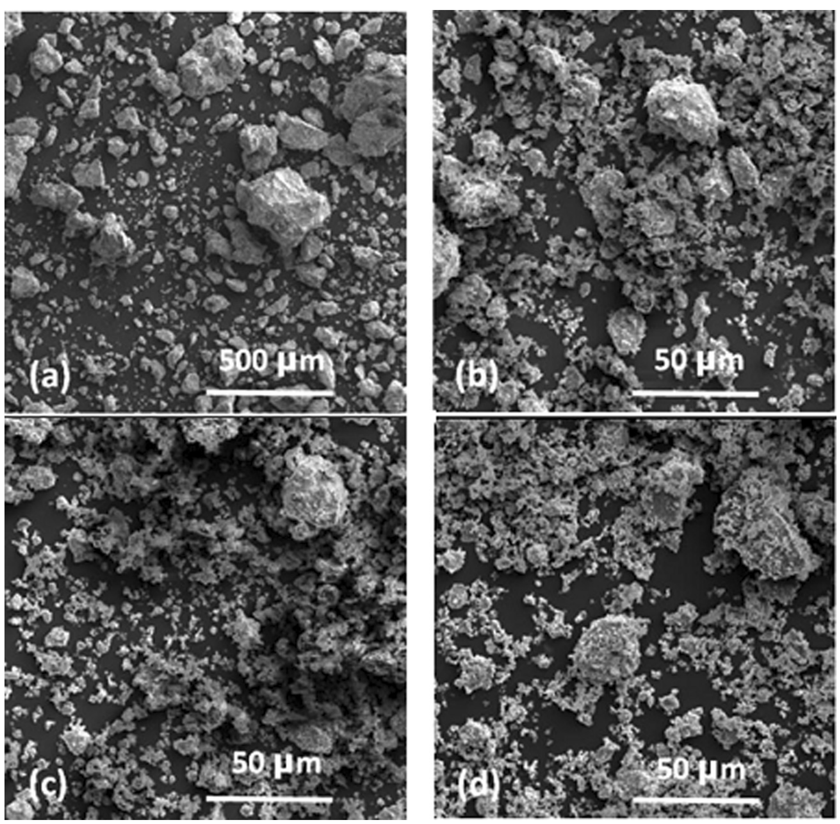

FIGURE 5.—SEM images of the powders prepared by combining the solid state reaction and ball milling processes (a) 0 h, (b) 2 h, (c) 7.5 h, and (d) 10 h.

Table 2.— The specification of the prepared powders

Method	Milling time (hr)	Particle size (μm)	Mean crystallite size (nm)	Lattice strain (%)	Main Phases
Mechanical alloying	0	0–500	—	—	2Mg+9Ni+Y
	5	30–100	37	0.371	Ni (Mg, Y) +Ni, Mg, and Y compounds
	10	5–30	31	0.428	
	20	5–20	18	0.650	Amorphous
	25	15–30	11	1.150	Amorphous
Solid state reaction and ball milling	0	20–300	—	—	Ni, Mg_2Ni_9Y, YNi_5, Y_2Ni_{17}, YNi_2, and YNi_4
	2	5–25	31	0.420	Ni, Mg_2Ni_9Y, YNi_5, Y_2Ni_{17}, and YNi_4
	10	2–15	19	0.625	Ni, Mg_2Ni_9Y, YNi_5, and Y_2Ni_{17}

and ball milling processes for 10 h is 39% smaller than that of the powders prepared only by the mechanical alloying at the same condition.

Alloying atoms or gaseous atoms, such as H, can readily diffuse to grain boundaries and then to the inside of the grains. The smaller the crystallite size, the higher the volume of the grain boundaries. Hence, smaller crystallite sizes can improve atomic diffusion and hence the reaction kinetics of gas-solid reactions.

Moreover, the lattice strain value created in the solid state reacted sample during 10 h of ball milling is 31.5% higher than that created in the sample prepared by only the mechanical alloying using the same milling condition. The lattice strain values increase with milling time due to the increase of the defects density in the microstructure, such as dislocations, vacancies, and grain boundaries, created by the plastic deformation and the shear impact during the ball milling. High densities of defects assist the diffusion of the gaseous atoms to the structure; therefore, they enhance the catalytic reaction kinetics in some reactions like sorption properties of the solid state hydrogen storage alloys.

Discussion

It can be seen in Table 2 that solid state reaction and subsequent mechanical milling can provide some special phases with fine particle sizes and high lattice strain values, the formation of which was not possible only by the mechanical alloying process. According to Table 2, the time required for preparing the samples with the same powder specifications through combining solid state reaction and ball milling processes is about 50% less than that required by only mechanical milling.

Conclusions

The following conclusions were drawn from the results of the present study:

1. Some ternary and binary phases such as Mg_2Ni_9Y, YNi_5, and Y_2Ni_{17} formed during solid state reaction and ball milling processes; however, these phases are not detectable in the powders prepared only by the mechanical alloying process due to their small amounts.
2. The particle sizes of the powders obtained by the mechanical alloying method reached 5 to 30 μm after 10 h of ball milling while the particle size of the powders obtained by combining solid state reaction and ball milling processes method reached 2 to 15 μm using the same milling condition. On the other hand, the particle sizes of the powders prepared by combining solid state reaction and ball milling processes were 50% smaller than that of the powders prepared by the mechanical alloying.
3. The crystallite size and lattice strain values of the particles processed by both solid state reaction and ball milling processes are, 39% smaller and 31.5% higher than those of the particles obtained from mechanical milling method, respectively.
4. Solid state reaction combined with mechanical milling can provide powders with smaller particles (i.e., higher surface areas and more reaction sites), smaller crystallite sizes (i.e., higher volume boundaries and more diffusion paths) and higher lattice strain (i.e., higher defects density and more diffusion paths), the formation of which is not possible only by the mechanical alloying process. Therefore, it is expected that solid state reaction and subsequent mechanical milling provide the powders with better catalytic specifications than the powders prepared by mechanical alloying.

References

1. Suriyranayana, C. *Mechanical Alloying and Milling*; Marcel Dekker Publications: New York, 2004.
2. Varin, R.A.; Zujko, C. Overview of processing of nanocrystalline hydrogen storage intermetallics by mechanical alloying/milling. *Materials and Manufacturing Processes* **2002**, *17* (2), 129–156.
3. Chawla, V.; Prakash, S.; Sidhu, B.S. State of the Art: Applications of mechanically alloyed nanomaterials—A review. *Materials and Manufacturing Processes* **2007**, *22* (4), 469–473.
4. Kadir, K.; Sakai, T.; Uehara, I. Structural investigation and hydrogen capacity of YMg_2Ni_9 and $(Y_{0.5}Ca_{0.5})(MgCa)Ni_9$: New phases in the AB_2C_9 system isostructural with $LaMg_2Ni_9$. *J. Alloys and Compounds* **1999**, *287*, 264–270.
5. Rothenberg, G. *Catalysis Concepts and Green Applications*; Wiley-VCH: Weinheim, Germany, 2008.
6. Moser, W.R. *Advanced Catalysts and Nanostructured Materials: Modern Synthesis Methods*; Academic Press: California, 1996.
7. Varin, R.A.; Czujko, T.; Wronski, Z.S. *Nanomaterials for Solid State Hydrogen Storage*; Springer Science: New York, 2009.
8. Walker, G. *Solid-State Hydrogen Storage Materials and Chemistry*; Woodhead Publishing Limited: Cambridge, UK, 2008.

9. Kadir, K.; Sakai, T.; Uehara, I. Synthesis and structure determination of a new series of hydrogen storage alloys; RMg_2Ni_9 (R = La, Ce, Pr, Nd, Sm and Gd) built from $MgNi_2$ laves-type layers alternating with AB_5 layers. *J. Alloys and Compounds* **1997**, *257*, 115–121.
10. Nakhl, M.; Chevalier, B.; Bobet, J.; Darriet, B. Structural and hydriding properties of the intermetallic $Y_{1-x}Ni_2$ synthesized by mechanical alloying or submitted to mechanical grinding. *J. Alloys and Compounds* **2001**, *314* (1–2), 275–280.
11. Stan, C.; Andronescu, E.; Predoi, D.; Bobet, J. Structural and hydrogen absorption/desorption properties of $YNi_{4-x}Al_xMg$ compounds (with $0 \leq x \leq 1.5$). *J. Alloys and Compounds* **2008**, *461*, 228–234.
12. Tuncel, S.; Roquefere, G.; Stan, C.; Bobet, L.; Chevalier, B.; Gaudin, E.; Hoffmann, D.; Rodewald, U.; Pottgen, R. Rare earth metal rich magnesium compounds RE_4NiMg (RE = Y, Pr–Nd, Sm, Gd–Tm, Lu)-Synthesis, structure, and hydrogenation behavior. *Solid State Chemistry* **2009**, *182*, 229–235.
13. Kalinichenka, S.; Röntzsch, L.; Kieback, B. Structural and hydrogen storage properties of melt-spun Mg–Ni–Y alloys. *Int. J. Hydrogen Energy* **2009**, *34* (18), 7749–7755.
14. Williamson, G.K.; Hall, W.H. X-ray line broadening from filed aluminum and wolfram. *Acta Metallurgica* **1953**, *1*, 22–31.
15. Mezbahul-Islam, M.; Medraj, M. A critical thermodynamic assessment of the Mg–Ni, Ni–Y binary and Mg–Ni–Y ternary systems. *Calphad* **2009**, *33*, 478–486.
16. Zhao, H.D.; Qin, G.W.; Ren, Y.P.; Pei, W.L.; Chen, D.; Guo, Y. The maximum solubility of Y in α -Mg and composition ranges of $Mg_{24}Y_{5-x}$ and Mg_2Y_{1-x} intermetallic phases in Mg–Y binary system. *J. Alloys and Compounds* **2011**, *509*, 627–631.
17. Ran, Q.; Lukas, H.L.; Effenburg, G.; Petzew, G. Thermodynamic optimization of the Mg-Y system. *Calphad* **1988**, *12* (4), 375–381.